arXiv:2601.16322v2 [cond-mat.quant-gas] 11 Jun 2026

# Controlled Switching of Bose-Einstein Condensation in a Mixture of Two Species of Polaritons

Hassan Alnatah,[1] Shuang Liang,[2,*] Qiaochu Wan,[2] Jonathan Beaumariage,[2]
Kirk Baldwin,[3] Adbhut Gupta,[3] Loren N. Pfeiffer,[3] and David W. Snoke[2]

[1] *Joint Quantum Institute, University of Maryland, 4254 Stadium Dr., College Park, Maryland 20742, USA*
[2] *Department of Physics, University of Pittsburgh, 3941 O'Hara Street, Pittsburgh, Pennsylvania 15218, USA*
[3] *Department of Electrical Engineering, Princeton University, Princeton, New Jersey 08544, USA*

(Dated: June 12, 2026)

We report temperature-dependent switching between lower and upper polariton condensation in a GaAs/AlGaAs microcavity when both of these species have comparable populations in a mixture. Using angle-resolved photoluminescence, we observe that at low temperatures, condensation occurs in the lower polariton branch, while at elevated temperatures, the upper polariton branch can become favored. At an intermediate temperature, we observe instability in the condensate formation, characterized by metastable correlations of the fluctuations in intensity and linewidth of the lower and upper polariton branches.

## I. INTRODUCTION

Exciton-polaritons are quasiparticles formed by the strong coupling of semiconductor quantum well excitons and cavity photons [1]. Polaritons can be viewed as photons dressed with an effective mass and repulsive interactions, making them ideal candidates for studying Bose-Einstein condensation (BEC) [2–9] and for nonlinear optical devices [10–12].

Over the past two decades, polariton condensation has been primarily observed in the lower polariton (LP) branch, where favorable relaxation dynamics allow efficient scattering to the ground state [13, 14]. In contrast, the upper polariton (UP) branch, which is at higher energy, has rarely been associated with condensation, primarily due to low thermal population at low temperatures and the efficient conversion of UP to LP by emitting optical phonons. Recent experimental advances, however, have enabled the observation of condensation in the UP branch under specific conditions [15]. This result challenges the conventional assumption that polariton condensation is strictly confined to the LP state, and opens the door to exploring the complex landscape of condensate mode competition.

Recent theoretical work has predicted that under non-equilibrium conditions, condensation can occur in the UP branch due to a non-Hermitian phase transition between polariton BEC and photon lasing [16]. In particular, Hanai et al. showed that bistability and switching between LP and UP condensates can occur near an exceptional point. Our results provide direct experimental evidence for this behavior, revealing temperature-induced switching and temporal fluctuations between LP and UP condensation near threshold. In many ways, this work is also analogous to BEC in multi-species systems in cold atoms gases (e.g., Refs. [17–19]), but with free interconversion between the species.

Mode competition and switching have been studied extensively in driven-dissipative polariton condensates, including optical bistability [20], polariton multistability [21, 22], fluctuation-driven switching near bistable points [23], critical fluctuations near the condensation threshold [24], and temporal fluctuations of $g^{(2)}$ near threshold characterized by stochastic hopping between condensed and non-condensed states [25]. Here, we report a different kind of switching: not between two states of the same branch, but between two condensate states on two distinct polariton branches.

In this work, we use the temperature of the cryostat bath to tune switching between condensation in the LP and UP branches in a GaAs/AlGaAs microcavity system. By tuning the lattice temperature, we observe that LP condensation is favored at low temperatures and switches to UP condensation at high temperatures. At a specific intermediate temperature around 80 K, the condensate displays stochastic switching behavior, alternating between the two branches even under identical experimental conditions. This behavior suggests that the system enters a regime of competing condensate states near the condensation threshold, where small fluctuations in carrier dynamics or relaxation pathways can determine the dominant condensate mode.

In addition to its fundamental interest, controllable switching between lower- and upper-polariton condensation has direct implications for polariton-based photonic devices. The ability to select the condensate branch using a temperature control provides a new mechanism for realizing bistable coherent light sources in a medium with strong nonlinearity.

* H.A. and S.L. contributed equally to this work.; address correspondence to: SHL450@pitt.edu

## II. EXPERIMENTAL METHODS

In the experiments reported here, we used a GaAs/AlGaAs microcavity structure very similar to those of previous experiments [26–28]. The microcavity sample consisted of a total of 12 GaAs quantum wells with AlAs barriers embedded within a distributed Bragg reflector (DBR). The DBRs are made of alternating layers of AlAs and $Al_{0.2}Ga_{0.8}As$. The top DBR is composed of 23 pairs and the bottom DBR is composed of 40 pairs. The quantum wells are in groups of four, with each group placed at one of the antinodes of cavity. A schematic illustration of the sample structure is provided in the Supplementary Material. A key feature of the experiments described here is that they were performed using a sample with a lower Q factor than the highest-quality samples available. For the very high-$Q$ samples used in previous works (e.g., [29–31]), the scattering from UP to LP is faster than the decay rate, making the UP hard to detect. As the cavity lifetime is decreased, it becomes comparable to the time for conversion from UP to LP, so that we can easily see the dynamics of the two populations competing for condensation. We therefore used a variation with $Q$ nominally equal to $\sim 4 \times 10^4$.

The sample was placed in a variable-temperature microscope cryostat, and the polaritons were generated by non-resonantly exciting the sample with a wavelength-tunable continuous wave laser, set to a reflectivity minimum (719.2 nm) approximately 172 meV above the lower polariton resonance. To minimize heating of the sample, the pump was modulated using an optical chopper operating at a 1% duty cycle, producing pulses of roughly 25 $\mu$s–much longer than the intrinsic timescales of the polariton dynamics. The non-resonant pump excitation created electron-hole pairs, which relaxed in energy and formed polaritons. The photoluminescence (PL) was collected using a microscope objective with a numerical aperture of 0.75 and was imaged onto the entrance slit of a spectrometer. The image was then sent through the spectrometer to a CCD camera for time-integrated imaging.

To measure the energy dispersion of the polaritons, we used angle-resolved photoluminscence (PL) to obtain the intensity image $I(\theta, E)$, where $\theta$ is the angle of emission, which has a one-to-one mapping to the in-plane momentum of the polaritons. The angle of photon emission maps directly to the in-plane $k$-vector of the particles inside the structure [32–34].

## III. EXPERIMENTAL RESULTS

Figure S4 shows examples of dispersion of the polaritons measured at two different temperatures, clearly demonstrating strong coupling with two distinct polariton branches. These branches, lower-polariton (LP) and upper-polariton (UP), arise due to the interaction between the heavy-hole exciton with the cavity photon

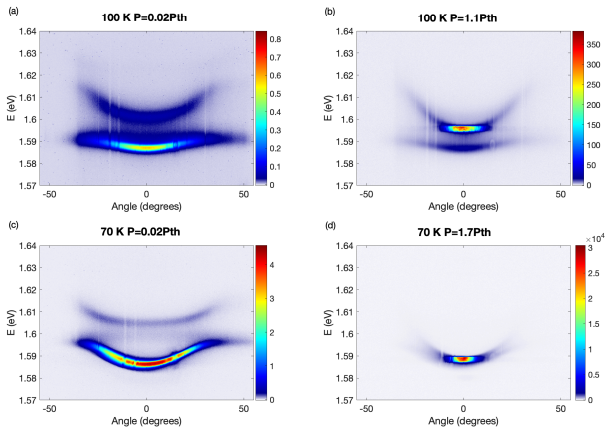



Figure 1: **Energy-resolved PL at 100 K and 70 K. (a)** angle-resolved PL measurements of the polariton at very low pumping power with a LP exciton fraction of 0.51 and **(b)** high pumping power at 100 K. (c,d) angle-resolved PL measurements at 70 K and LP exciton fraction 0.22 under low (c) and high (d) pumping conditions.

mode. (At high temperature, the light-hole exciton comes into play, as discussed in Ref. [27], but here can be ignored.)

As the pump power is increased across the condensation threshold, polariton condensation was observed. Figure S4 shows angle-resolved PL at low and high pumping powers for each temperature. Consistent with typical condensation behavior, the PL narrows both in $k$-space and in energy width as the density increases; the latter indicates coherence of the emission [35–38].

We find that branch which condenses first depends on both the temperature and the exciton fraction. At a lattice temperature of 100 K, the polaritons condense in the upper polariton branch when the exciton fraction of the LP is 0.51, as shown in Fig. S4(b). In contrast, at 70 K and a LP exciton fraction of 0.22, condensation occurs in the lower branch, as seen in Fig. S4(d). This temperature-dependent switching between upper and lower branch condensation highlights the sensitivity of the system to thermal and relaxation dynamics, as well as the exciton fraction which sets the masses of both branches. For these detunings, at 70 K, the lower polariton branch is favored, which lies at a lower energy and typically hosts the condensate under standard conditions. However, at 100 K, the increased thermal population allows condensation to instead occur in the upper branch despite its higher energy. Further quantitative analysis of the PL lines is presented in the Supplementary Material (Figs. S2 and S3).

Notably, for some values of temperture and exciton fraction (in this case $80 \pm 2$ K and exciton fraction 0.68), we find that the polariton system exhibits an instability in mode selection precisely at the condensation threshold.

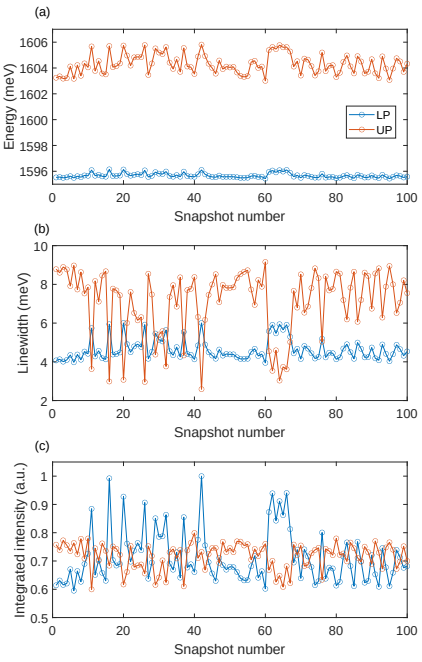



Figure 2: **Anticorrelated coherence at a fixed power and temperature (80 K)**, for LP exciton fraction of 0.68, near the condensation threshold. **(a)** The energy, (b) the linewidth and (c) the maximum intensity as a function on snapshot number.

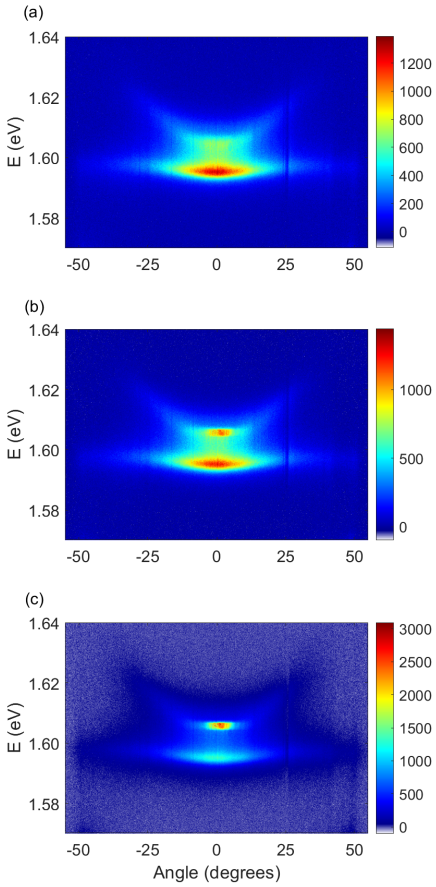



Figure 3: **Selected snapshots at fixed temperature of 80 K**, for LP exciton fraction of 0.68 and pump power corresponding to Fig. 2, for identical experimental conditions. **(a)** The LP is brighter, **(b)** the LP and UP have the same brightness, **(c)** the UP is brighter. The exciton fraction of the LP is 0.68.

That is, the polaritons appear to fluctuate between condensation in the UP and LP branches, as if they cannot "decide" which state to macroscopically occupy.

To study this behavior, we took a series of snapshots of the PL, where each snapshot was time integrated for 100 ms and represents an average over 40 laser pulses. Despite identical experimental conditions across snapshots, the system displays fluctuations in both linewidth and intensity, alternating between the LP and UP branches as shown in Fig. 2. Interestingly, the system shows an an anticorrelated switching behavior, where the linewidths and integrated intensity of the LP and UP branches vary in opposite directions.

Figure 3 shows selected angle-resolved photoluminescence images taken under identical experimental conditions, illustrating the underlying fluctuations that give rise to the statistical data shown in Fig. 2. Each panel represents a single 100 ms time-integrated snapshot and highlights a different realization of the condensate behavior. In some instances, the emission is dominated by the lower polariton (LP) branch (Fig. 3 (a)), indicating that condensation has occurred predominantly in the LP state. In other cases, the upper polariton (UP) branch is significantly brighter (Fig. 3 (c)), suggesting that the condensate has formed in the higher-energy UP state, and in some cases, both branches exhibit comparable brightness, indicating either rapid switching between the two which is averaged in our time-integrated measurements, or coexistence between LP and UP condensation (Fig. 3(b)).

We note that the condensate does not have the same degree of coherence in the LP and UP branches when this instability occurs. As seen in Fig. 2, the UP condensate, when it exists, has quite narrow spectral line, while the LP condensate has a typical full width at half maximum of 4 meV. This is narrower than its width when the UP is condensed, indicating that the LP in this case is a "quasicondensate" with an increased degree of coherence, but not a fully coherent condensate. Also, we note that while the UP condensate is narrower, its energy position is more unstable.

To further quantify the condensation behavior, we extracted the average linewidth and intensity by integrating the PL signal over many laser pulses (typically more

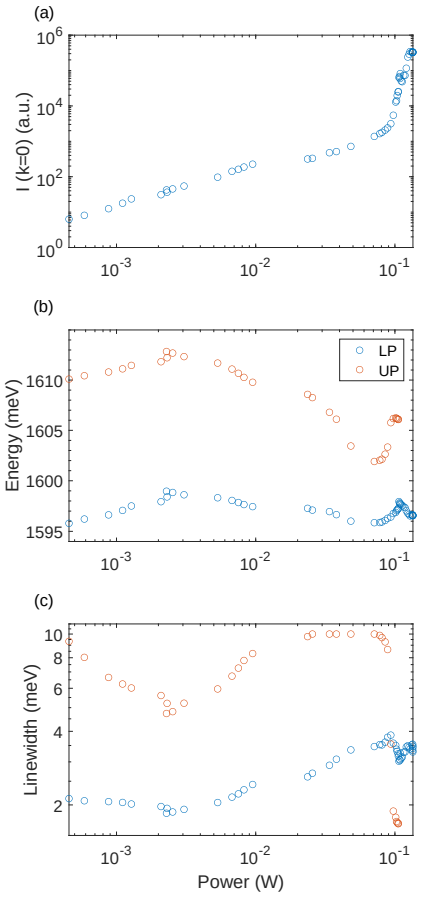



Figure 4: **Characteristics of the PL lines at 80 K**, averaged over many shots as in the data of Figure 2. **(a)** The intensity at $k = 0$ of the polaritons as a function of pump power. **(b)** The energies of the polariton lines at $k = 0$ as a function of the pump power. **(c)** Full width at half maximum at $k = 0$.

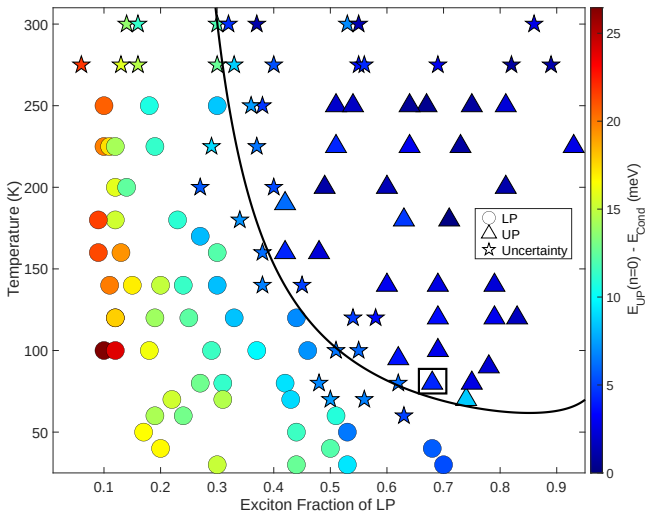



Figure 5: **Phase diagram** showing the LP exciton fraction versus temperature for LP and UP condensates. The exciton fraction for various locations on the microcavity sample has been deduced using fits to the energies $E_{LP}(\theta)$ and $E_{UP}(\theta)$ from data like that shown in Figure S4 at low pump density, using a model like that of Eq. (2) but with three levels for the photon, heavy-hole exciton and light-hole exciton in GaAs quantum wells. Triangles represent conditions where condensation occurs in the upper polariton branch, while circles represent condensation in the lower polariton branch. The color bar gives the emission energy of the condensate relative to the zero-density upper polariton branch. The symbol with the square gives the conditions of the metastable jumping between the different states seen in Figures 2 and 3. The solid black line is given by Eq. (6) for the parameters given in the text.

than 480) at a temperature of 80 K, corresponding to the same data as in Figs. 2 and 3. In these plots, the data from multiple shots is averaged. Near the condensation threshold, a nonlinear increase in intensity is observed. This sharp increase in intensity is accompanied by a decrease in the line width of the UP by approximately a factor of 10.

Finally, in Figure 5, we plot a phase diagram of sorts. All of the symbols represent conditions in which we can clearly identify the upper and lower polariton energies at low density. The shape of the symbol indicates whether the condensate, when it appears, occurs in the lower or upper polariton state. Stars indicate conditions in which we can see only one line when the system is a condensate, so that we cannot clearly identify it as either the upper or lower branch. The color of the symbols gives the energy of the condensate relative to the upper branch energy at low density. As seen in the figure, the condensate forms in whichever branch is more photonic, and therefore has lighter effective mass. When the lower polariton is photon-like (low exciton fraction), condensation occurs in the lower branch; when the lower polariton is exciton-like (high exciton fraction), the upper polariton is the more photonic branch and condensation occurs there instead. There is a temperature threshold, however, around 70 K, below which the condensation is in the lower polariton state for all detunings. This plot does not include data for very low temperature, where the condensate is in the lower branch, but we cannot observe the UP branch at those low temperatures, because there is not sufficient thermal occupation to give PL from the upper state.

We emphasize that the condensates represented in Fig. 5 remain in the strong-coupling regime across these conditions. To rule out a transition to weak-coupling photon lasing at high density, we performed spatially resolved measurements isolating the homogeneous center

of the pump spot at representative temperatures of 80 K and 100 K (shown in the SI file). Even when the PL collection is restricted to only the very center of the condensate, the lower polariton branch is seen to retain its characteristic curvature and coexists with the upper polariton condensate, confirming that strong coupling persists at the condensation threshold.

## IV. DISCUSSION

Although the UP state is disfavored for condensation because it is not the ground state, if the conversion between the populations of the UP and LP states is slow, and the UP state has lighter effective mass, the quantum degeneracy of the UP state can be greater than that of the LP, allowing condensation to appear there first.

A simple model predicts whether a condensate will appear first in the LP or UP state. We assume that the two populations have a slow, but nonzero interconversion between them. In this case, we can take the relative total population of the two as just given by the Boltzmann factor for the energy difference between them, $\exp(-\Delta E_0/k_BT)$. Within each population, we then assume fast interactions that allow each population to become a BEC based only on that population's density and temperature. Clearly, if there is fast interconversion between the populations, the condensate will always appear in the overall ground state, in the lower polariton. But out of equilibrium, this model of separation of time scales predicts that either can become a BEC first, after which the BEC in that population will alter the rate of interconversion, stimulating particles to enter the BEC, making that BEC metastable. Below, we calculate the crossover point for BEC in the two different states, based on this model. As shown by the solid line in Fig. 5, it gives a remarkably good fit to the data.

The quantum degeneracy of each population is proportional to its total density divided by its density of states, which is proportional to its effective mass in a two-dimensional gas. If we assume that initially the ratio of the LP and UP total populations is given by a Boltzmann thermal factor, then the ratio of the degeneracies will be

$$\frac{N_{\rm UP}}{N_{\rm LP}} = \frac{m_{\rm LP}}{m_{\rm UP}} \exp\left(-\frac{\Delta E_0}{k_BT}\right), \tag{1}$$

where $N_{LP}$ and $N_{UP}$ are the typical occupation numbers of the ground state of the LP and UP states, respectively, the masses and ground-state energies of the two populations are labeled accordingly, and $\Delta E_0 \equiv E_{\rm UP}(0) - E_{\rm LP}(0)$. The crossover between UP and LP condensation will occur when this factor equals 1.

To calculate $\Delta E_0$ and the mass ratio of the two species, we assume a simple two-level system for the polaritons [33], with a coupling Hamiltonian given by

$$H(k=0) = \begin{pmatrix} E_{\rm phot}(0) & \Omega/2 \\ \Omega/2 & E_{\rm exc}(0) \end{pmatrix} \tag{2}$$

where $E_{\rm phot}(0)$ and $E_{\rm exc}(0)$ are the bare cavity photon and bare exciton energies at $k = 0$, respectively, and $\Omega$ is the Rabi coupling energy. Diagonalization of this matrix gives

$$E_{\rm UP}(0) - E_{\rm LP}(0) = \sqrt{\Delta_0^2 + \Omega^2}, \tag{3}$$

which can be expressed as a function of the exciton fraction $|X^{\rm LP}|^2$ as

$$\Delta_0 = \Omega \frac{2|X^{\rm LP}|^2 - 1}{2\sqrt{|X^{\rm LP}|^2\left(1 - |X^{\rm LP}|^2\right)}}. \tag{4}$$

The exciton fraction $f_{ex}^{\rm LP} = |X^{\rm LP}|^2$, in turn, is defined from the eigenvectors of the Hamiltonian, $|{\rm LP}\rangle = C^{\rm LP}|{\rm phot}\rangle + X^{\rm LP}|{\rm ex}\rangle$ and $|{\rm UP}\rangle = C^{\rm UP}|{\rm phot}\rangle + X^{\rm UP}|{\rm ex}\rangle$, where $X$ and $C$ are the Hopfield coefficients [39].

The effective masses are deduced from (2) when an additional term $\hbar^2 k_\parallel^2/2m_{\rm cav}$ is added to $E_{\rm phot}(0)$, where $m_{\rm cav}$ is the effective mass of the bare cavity photon mode, and $k_\parallel$ is the in-plane momentum, equal to $k\sin\theta$. These can be expressed in terms of the exciton and photon fraction, which in the limit $m_{\rm ex} \gg m_{\rm cav}$ can be written as

$$\frac{1}{m_{\rm LP}} \approx \frac{|C^{\rm LP}|^2}{m_{\rm cav}}, \qquad \frac{1}{m_{\rm UP}} \approx \frac{|X^{\rm LP}|^2}{m_{\rm cav}}. \tag{5}$$

We now suppose that upper polariton condensation will occur when the degeneracy ratio (1) is greater than 1, by some factor. Putting everything together, we have

$$\begin{aligned} \frac{N_{\rm UP}}{N_{\rm LP}} &= A\frac{|X^{\rm LP}|^2}{|C^{\rm LP}|^2} \exp\left(-\frac{\sqrt{\Delta_0^2 + \Omega^2}}{k_BT}\right) \\ &= A\frac{|X^{\rm LP}|^2}{1 - |X^{\rm LP}|^2} \exp\left(-\frac{\sqrt{\Delta_0^2 + \Omega^2}}{k_BT}\right), \end{aligned} \tag{6}$$

where $A$ is the threshold ratio for upper polariton condensation.

The implications of Eq. (6) can be understood by first considering the limit where the two species are completely decoupled, with separately conserved particle numbers and no exchange between them. In that case, each branch independently reaches the 2D quantum-degenerate condition when $n_i \gtrsim m_i k_B T/\hbar^2$ as the temperature is lowered. If the populatiopns of the two branches are equal, the branch with the smaller effective mass reaches the threshold first, independent of the energy offset between them, since $\Delta E_0$ plays no role without thermal exchange.

Equation (6) extends beyond this limit by incorporating the tendency for condensation to occur in the lower-energy state. This competition is captured by the Boltzmann factor $\exp\left(-\sqrt{\Delta_0^2 + \Omega^2}/k_BT\right)$, which always remains smaller than unity and therefore favors occupation of the lower-energy LP branch. In contrast, the Hopfield prefactor $|X^{\rm LP}|^2/|C^{\rm LP}|^2 = m_{\rm LP}/m_{\rm UP}$ can become larger than one when the UP becomes sufficiently photonic and

light, favoring UP condensation through its smaller critical density. As a result, the product of these two factors can become either smaller or larger than unity depending on the relative balance between the energy splitting and the mass ratio. At low temperatures, however, the Boltzmann factor becomes exponentially small and can no longer be compensated by the mass difference, leading to condensation always in the LP branch. The competition between the lower LP energy and the lighter UP mass defines the phase boundary in Fig. 5.

The data (e.g., Figure 4) shows that the Rabi splitting $\Omega$ decreases as the density increases, as expected due to Pauli phase-space filling (see, e.g., [40–42]). Since higher temperature requires high density for condensation, approximately given by $n_c = mk_BT/\hbar^2$ in two dimensions, we assume the Rabi coupling that enters into (6) has form $\Omega = \Omega_0(1 - \alpha n_c)$, where $n_c$ is computed using an average effective mass $m = (1/m_{\mathrm{LP}} + 1/m_{\mathrm{UP}})^{-1} = m_{\mathrm{cav}}$.

The model has two fit parameters, which are $A$ and $\alpha$. The effective mass of the states and the zero-density splitting are directly measured, which are given by $\Omega_0 =$ 12 meV and $m_{\mathrm{cav}} = 4 \times 10^{-5} m_e$. The solid line in Figure 5 corresponds to $A = 3$ and $\alpha = 0.037\ \mu\mathrm{m}^2$. As seen in this figure, the predicted phase boundary gives quite good agreement with the experimental results. Note that although Figure 5 does not show data from other experiments, all prior experiments using microcavity samples with this design show only LP condensation when $T < 50$ K.

## V. CONCLUSIONS

We have demonstrated temperature-dependent switching of polariton condensation between two different species of polaritons in a GaAs/AlGaAs microcavity. Remarkably, a simple model of the relative degeneracy of the two states predicts the phase diagram of this switching without needing to refer to drive-dissipative dynamics such as pumping and decay rates. Essentially, when the two mixed species have slow interconversion and roughly equal population, whichever has the lighter mass will condense, because it will have greater quantum degeneracy.

Near 80 K, the system exhibits an instability in condensate formation, with stochastic switching between branches under the same pumping power. This points us to explore the critical dynamics near the phase transition leading to mode switching, similar to that seen in prior work with much lower energy difference between the stable modes [24, 25].

The behavior we see indicates that the switching between the two condensate states is hypersensitive to the parameters of the experiment when the system is at the phase boundary. Therefore, this phenomenon could potentially be adapted for nonlinear switching applications, for example, using short, weak laser pulses to push the system over the phase boundary between UP and LP condensation.

## VI. ACKNOWLEDGMENTS

This project has been supported by the National Science Foundation grant DMR-2306977. We thank M. Szymanska and P. Comaron for helpful conversations.

## REFERENCES


[1] C. Weisbuch, M. Nishioka, A. Ishikawa, and Y. Arakawa, Observation of the coupled exciton-photon mode splitting in a semiconductor quantum microcavity, Physical review letters **69**, 3314 (1992).

[2] H. Deng, G. Weihs, C. Santori, J. Bloch, and Y. Yamamoto, Condensation of semiconductor microcavity exciton polaritons, Science **298**, 199 (2002).

[3] J. Kasprzak, M. Richard, S. Kundermann, A. Baas, P. Jeambrun, J. M. J. Keeling, F. Marchetti, M. Szymańska, R. André, J. Staehli, *et al.*, Bose–Einstein condensation of exciton polaritons, Nature **443**, 409 (2006).

[4] R. Balili, V. Hartwell, D. Snoke, L. Pfeiffer, and K. West, Bose-Einstein condensation of microcavity polaritons in a trap, Science **316**, 1007 (2007).

[5] M. Abbarchi, A. Amo, V. Sala, D. Solnyshkov, H. Flayac, L. Ferrier, I. Sagnes, E. Galopin, A. Lemaître, G. Malpuech, *et al.*, Macroscopic quantum self-trapping and Josephson oscillations of exciton polaritons, Nature Physics **9**, 275 (2013).

[6] D. Sanvitto, F. Marchetti, M. Szymańska, G. Tosi, M. Baudisch, F. P. Laussy, D. Krizhanovskii, M. Skolnick, L. Marrucci, A. Lemaitre, *et al.*, Persistent currents and quantized vortices in a polariton superfluid, Nature Physics **6**, 527 (2010).

[7] K. Lagoudakis, T. Ostatnickỳ, A. Kavokin, Y. G. Rubo, R. André, and B. Deveaud-Plédran, Observation of half-quantum vortices in an exciton-polariton condensate, Science **326**, 974 (2009).

[8] A. Amo, J. Lefrère, S. Pigeon, C. Adrados, C. Ciuti, I. Carusotto, R. Houdré, E. Giacobino, and A. Bramati, Superfluidity of polaritons in semiconductor microcavities, Nature Physics **5**, 805 (2009).

[9] G. Nardin, G. Grosso, Y. Léger, B. Pięt̨ka, F. Morier-Genoud, and B. Deveaud-Plédran, Hydrodynamic nucleation of quantized vortex pairs in a polariton quantum fluid, Nature Physics **7**, 635 (2011).

[10] D. Sanvitto and S. Kéna-Cohen, The road towards polaritonic devices, Nature materials **15**, 1061 (2016).

[11] D. Ballarini, M. De Giorgi, E. Cancellieri, R. Houdré, E. Giacobino, R. Cingolani, A. Bramati, G. Gigli, and D. Sanvitto, All-optical polariton transistor, Nature communications **4**, 1778 (2013).

[12] A. Amo, T. Liew, C. Adrados, R. Houdré, E. Giacobino, A. Kavokin, and A. Bramati, Exciton–polariton spin switches, Nature Photonics **4**, 361 (2010).

[13] F. Tassone and Y. Yamamoto, Exciton-exciton scattering dynamics in a semiconductor microcavity and stimulated scattering into polaritons, Physical Review B **59**, 10830 (1999).

[14] D. Porras, C. Ciuti, J. Baumberg, and C. Tejedor, Polariton dynamics and bose-einstein condensation in semiconductor microcavities, Physical Review B **66**, 085304 (2002).

[15] X. Chen, H. Alnatah, D. Mao, M. Xu, Y. Fan, Q. Wan, J. Beaumariage, W. Xie, H. Xu, Z.-Y. Shi, *et al.*, Bose condensation of upper-branch exciton-polaritons in a transferable microcavity, Nano Letters **23**, 9538 (2023).

[16] R. Hanai, A. Edelman, Y. Ohashi, and P. B. Littlewood, Non-Hermitian phase transition from a polariton Bose-Einstein condensate to a photon laser, Physical Review Letters **122**, 185301 (2019).

[17] C. Frapolli, T. Zibold, A. Invernizzi, K. Jiménez-García, J. Dalibard, and F. Gerbier, Stepwise Bose-Einstein condensation in a spinor gas, arXiv preprint arXiv:1702.08265 (2017).

[18] D. M. Stamper-Kurn and M. Ueda, Spinor bose gases: Symmetries, magnetism, and quantum dynamics, Reviews of Modern Physics **85**, 1191 (2013).

[19] C. Myatt, E. Burt, R. Ghrist, E. A. Cornell, and C. Wieman, Production of two overlapping bose-einstein condensates by sympathetic cooling, Physical Review Letters **78**, 586 (1997).

[20] A. Baas, J. P. Karr, H. Eleuch, and E. Giacobino, Optical bistability in semiconductor microcavities, Physical Review A **69**, 023809 (2004).

[21] N. Gippius, I. Shelykh, D. Solnyshkov, S. Gavrilov, Y. G. Rubo, A. V. Kavokin, S. Tikhodeev, and G. Malpuech, Polarization multistability of cavity polaritons, Physical review letters **98**, 236401 (2007).

[22] T. Paraïso, M. Wouters, Y. Leger, F. Morier-Genoud, and B. Deveaud-Plédran, Erratum: Multistability of a coherent spin ensemble in a semiconductor microcavity, Nature Materials **10**, 80 (2011).

[23] S. Rodriguez, W. Casteels, F. Storme, N. Carlon Zambon, I. Sagnes, L. Le Gratiet, E. Galopin, A. Lemaître, A. Amo, C. Ciuti, *et al.*, Probing a dissipative phase transition via dynamical optical hysteresis, Physical review letters **118**, 247402 (2017).

[24] H. Alnatah, P. Comaron, S. Mukherjee, J. Beaumariage, L. N. Pfeiffer, K. West, K. Baldwin, M. Szymańska, and D. W. Snoke, Critical fluctuations in a confined driven-dissipative quantum condensate, Science Advances **10**, eadi6762 (2024).

[25] E. Rozas, W. Bukalski, Y. Brune, A. Gupta, K. Baldwin, L. N. Pfeiffer, H. Alnatah, J. Beaumariage, D. W. Snoke, P. Comaron, *et al.*, Temporal hopping dynamics in exciton-polariton condensation, arXiv preprint arXiv:2604.25519 (2026).

[26] H. Alnatah, S. Liang, Q. Yao, Q. Wan, J. Beaumariage, K. West, K. Baldwin, L. N. Pfeiffer, and D. W. Snoke, Bose–Einstein condensation of polaritons at room temperature in a GaAs/AlGaAs structure, ACS Photonics (2024).

[27] H. Alnatah, S. Liang, Q. Wan, J. Beaumariage, K. West, K. Baldwin, L. N. Pfeiffer, M. C. A. Tam, Z. R. Wasilewski, and D. W. Snoke, Strong coupling of polaritons at room temperature in a GaAs/AlGaAs structure, Physical Review B **112**, 045307 (2025).

[28] S. Liang, H. Alnatah, Q. Yao, J. Beaumariage, K. West, K. Baldwin, L. N. Pfeiffer, N. G. Berloff, and D. W. Snoke, Mirror-mediated long-range coupling and robust phase locking of spatially separated exciton-polariton condensates, arXiv preprint arXiv:2506.20924 (2025).

[29] M. Steger, C. Gautham, D. W. Snoke, L. Pfeiffer, and K. West, Slow reflection and two-photon generation of microcavity exciton–polaritons, Optica **2**, 1 (2015).

[30] B. Nelsen, G. Liu, M. Steger, D. W. Snoke, R. Balili, K. West, and L. Pfeiffer, Dissipationless flow and sharp threshold of a polariton condensate with long lifetime, Physical Review X **3**, 041015 (2013).

[31] H. Alnatah, Q. Yao, J. Beaumariage, S. Mukherjee, M. C. Tam, Z. Wasilewski, K. West, K. Baldwin, L. N. Pfeiffer, and D. W. Snoke, Coherence measurements of polaritons in thermal equilibrium reveal a power law for two-dimensional condensates, Science Advances **10**, eadk6960

(2024).
[32] I. Carusotto and C. Ciuti, Quantum fluids of light, Reviews of Modern Physics **85**, 299 (2013).
[33] H. Deng, H. Haug, and Y. Yamamoto, Exciton-polariton bose-einstein condensation, Reviews of Modern Physics **82**, 1489 (2010).
[34] R. Houdré, C. Weisbuch, R. Stanley, U. Oesterle, P. Pellandini, and M. Ilegems, Measurement of cavity-polariton dispersion curve from angle-resolved photoluminescence experiments, Physical Review Letters **73**, 2043 (1994).
[35] M. Richard, J. Kasprzak, R. André, R. Romestain, L. S. Dang, G. Malpuech, and A. Kavokin, Experimental evidence for nonequilibrium bose condensation of exciton polaritons, Physical Review B **72**, 201301 (2005).
[36] J. Kasprzak, M. Richard, A. Baas, B. Deveaud, R. André, J.-P. Poizat, and L. S. Dang, Second-order time correlations within a polariton bose-einstein condensate in a cdte microcavity, Physical Review Letters **100**, 067402 (2008).
[37] G. Roumpos, M. Lohse, W. H. Nitsche, J. Keeling, M. H. Szymańska, P. B. Littlewood, A. Löffler, S. Höfling, L. Worschech, A. Forchel, *et al.*, Power-law decay of the spatial correlation function in exciton-polariton condensates, Proceedings of the National Academy of Sciences **109**, 6467 (2012).
[38] Y. Brune, E. Rozas, K. West, K. Baldwin, L. N. Pfeiffer, J. Beaumariage, H. Alnatah, D. W. Snoke, and M. Aßmann, Quantum coherence of a long-lifetime exciton-polariton condensate, Communications Materials **6**, 123 (2025).
[39] J. Hopfield, Theory of the contribution of excitons to the complex dielectric constant of crystals, Physical Review **112**, 1555 (1958).
[40] J.-K. Rhee, R. Lai, T. Norris, Y. Arakawa, and M. Nishioka, Nonlinear vacuum Rabi splitting in semiconductor microcavities, in *Quantum Optoelectronics* (Optica Publishing Group, 1995) p. QThA3.
[41] R. Houdré, J. Gibernon, P. Pellandini, R. Stanley, U. Oesterle, C. Weisbuch, J. O'Gorman, B. Roycroft, and M. Ilegems, Saturation of the strong-coupling regime in a semiconductor microcavity: Free-carrier bleaching of cavity polaritons, Physical Review B **52**, 7810 (1995).
[42] S. Schmitt-Rink, D. Chemla, and D. A. Miller, Theory of transient excitonic optical nonlinearities in semiconductor quantum-well structures, Physical Review B **32**, 6601 (1985).

# Controlled Switching of Bose-Einstein Condensation in a Mixture of Two Species of Polaritons

Hassan Alnatah,[1] Shuang Liang,[2,*] Qiaochu Wan,[2] Jonathan Beaumariage,[2]
Kirk Baldwin,[3] Adbhut Gupta,[3] Loren N. Pfeiffer,[3] and David W. Snoke[2]

[1] *Joint Quantum Institute, University of Maryland, 4254 Stadium Dr., College Park, Maryland 20742, USA*
[2] *Department of Physics, University of Pittsburgh, 3941 O'Hara Street, Pittsburgh, Pennsylvania 15218, USA*
[3] *Department of Electrical Engineering, Princeton University, Princeton, New Jersey 08544, USA*

(Dated: June 12, 2026)

## I. SAMPLE DESIGN

The sample used in this work, as shown in Fig. S1, contained a total of 12 GaAs quantum wells (QWs) separated by AlAs barriers and embedded within a distributed Bragg reflector (DBR) microcavity with 23 pairs in the top DBR. All quantum wells had the same thickness and were arranged in groups of four, with each group positioned at an antinode of the cavity field. Furthermore, the DBRs consisted of alternating layers of AlAs and $Al_{0.2}Ga_{0.8}As$.

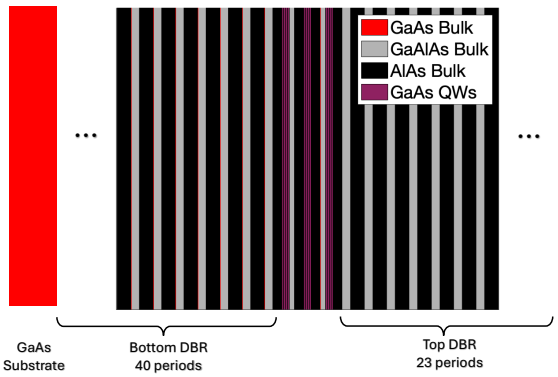



Figure S1: **Schematic illustration of the sample structure.** The GaAs quantum wells are embedded in a GaAs/AlGaAs microcavity formed by DBRs.

## II. CHARACTERISTICS OF PL LINES

Figures S2 and S3 show the power-dependent characteristics of the polariton emission at 100 K and 70 K, respectively. A clear threshold-like increase in the k=0 emission intensity is observed in Fig. S2(a). The UP branch exhibits a pronounced linewidth narrowing together with a characteristic change in its energy shift (see Figs. S2(b,c)), which are signatures commonly associated with polariton condensation. These data correspond to the measurements shown in Fig. 1(a,b) of the main text, obtained at 100 K, where the LP exciton fraction is approximately 0.51.

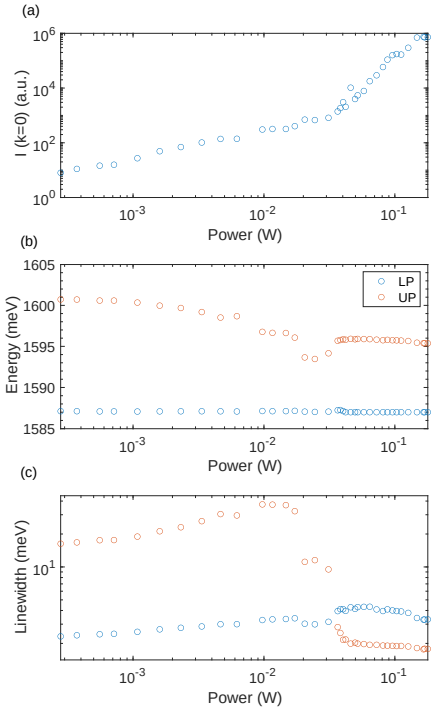



Figure S2: **Characteristics of the PL lines at 100 K.(a)** The intensity at $k = 0$ of the polaritons as a function of pump power. **(b)** The energies of the polariton lines at $k = 0$ as a function of the pump power. **(c)** Full width at half maximum at $k = 0$.

Figure S3 shows the power dependence of the LP photoluminescence at k=0. These data correspond to the same dataset shown in Fig. 1(c,d) of the main text, obtained at 70 K, where the LP exciton fraction is approximately 0.22. Because the upper-polariton (UP) mode at k=0 is predominantly excitonic at this detuning and therefore exhibits much weaker photoluminescence than

* H.A. and S.L. contributed equally to this work.; address correspondence to: SHL450@pitt.edu

the more photonic LP mode, only the LP emission is analyzed here. The LP emission exhibits a gradual blueshift together with linewidth reduction at elevated pump powers, indicating the onset of LP condensation. Thus, at 70 K the nonlinear behavior is associated with the LP branch rather than the UP branch. This behavior contrasts with that observed at 100 K, where condensation signatures predominantly appear in the UP branch, further supporting the temperature-dependent switching between LP and UP condensation.

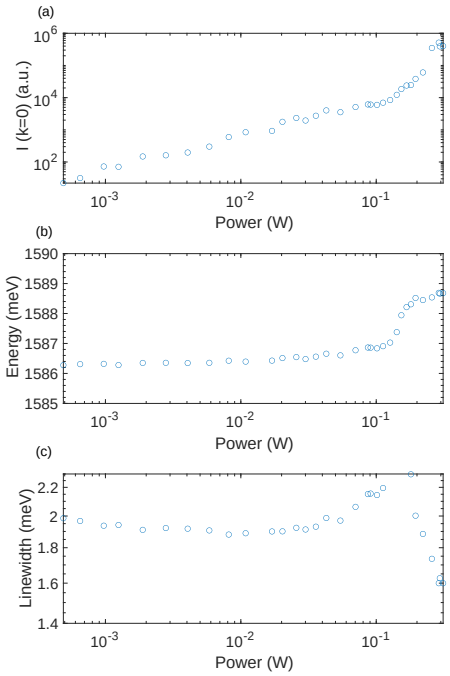



Figure S3: **Characteristics of the PL lines at 70 K. (a)** The intensity at $k = 0$ of the lower polariton as a function of pump power. **(b)** The energies of the lower polariton lines at $k = 0$ as a function of the pump power. **(c)** Full width at half maximum at $k = 0$.

## III. SPATIAL FILTERING

To address the concern that the emission at high density may originate from a transition to weak coupling (e.g. cavity phonon lasing) at the center of the pump spot—while strong coupling persists only in the outer regions—we performed spatially resolved measurements using a pinhole to isolate emission only from the pump center in a region that is spatially homogeneous.

As shown in Fig. S4(a–b), the PL was selected in real space using a pinhole of diameter 40 $\mu$m. The pinhole is not perfectly centered, as it was aligned with the brightest region of the condensate at the highest excitation power. Nevertheless, the intensity within the selected region remains sufficiently homogeneous.

With this spatial filtering, we clearly observe that the lower polariton branch remains visible even when upper polariton condensation occurs (see Fig. S4(d)). The data are plotted on a logarithmic scale to emphasize the lower polariton emission, since the upper polariton condensate is significantly brighter.

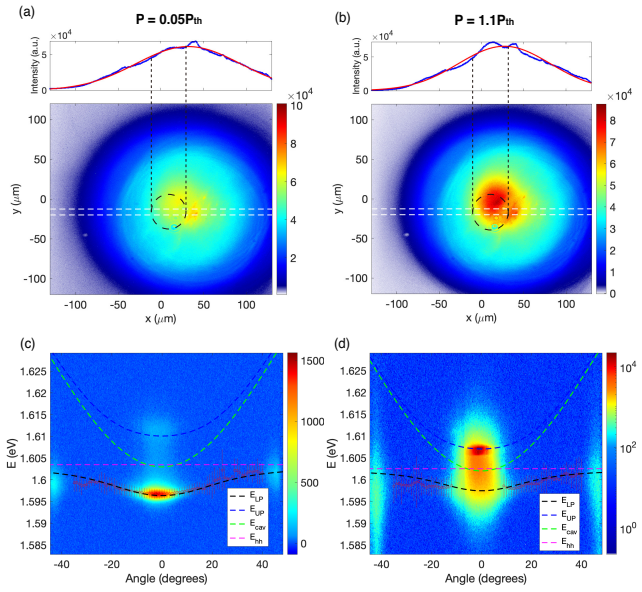



Figure S4: **Spatially and angle-resolved photoluminescence at 80 K for an exciton fraction of the lower polariton is 0.72. (a)** Real-space emission of polaritons at very low pumping power and **(b)** at high pumping power at 80 K. The black dashed circle indicates the position of the pinhole, with a diameter of approximately 40 $\mu$m. **(c,d)** Angle-resolved photoluminescence at the corresponding low and high pumping powers, respectively, after spatial filtering through the pinhole. The red circles represent the extracted dispersion, obtained by fitting each angle-resolved linecut with a Lorentzian. The dashed lines show fits to a two-level exciton-polariton model: the black line denotes the lower polariton branch, the blue line the upper polariton branch, the green line the cavity mode, and the magenta line the heavy-hole exciton.

Importantly, the lower polariton branch retains a finite curvature rather than appearing as a straight line, confirming that the system remains in the strong coupling regime. The markers shown in Fig. S4(c,d) are obtained by taking energy spectra at different emission angles and fitting the corresponding intensity $I(E)$ with a Lorentzian function to extract the peak positions. These extracted points clearly demonstrate that the lower polariton branch persists and coexists with the upper polariton condensate.

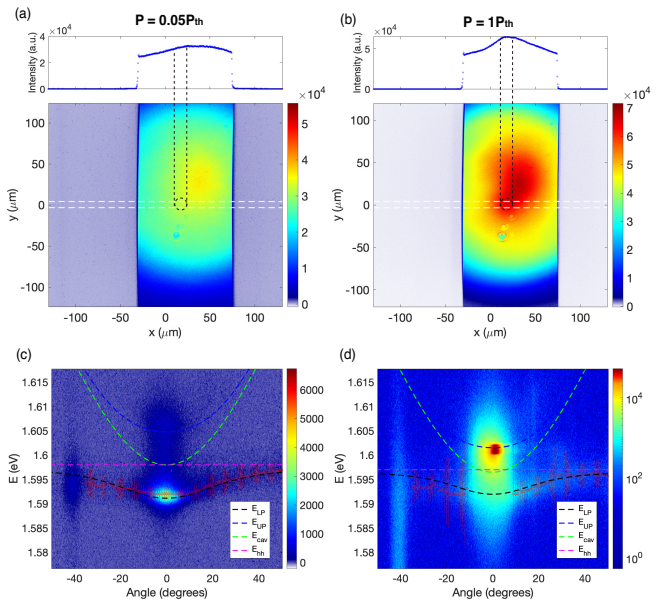



Figure S5: **Spatially and angle-resolved photoluminescence at 100 K for an exciton fraction of the lower polariton is 0.65. (a)** Real-space emission of polaritons at very low pumping power and **(b)** at high pumping power at 100 K. The black dashed circle indicates the position of the pinhole, with a diameter of approximately 10 $\mu$m. **(c,d)** Angle-resolved photoluminescence at the corresponding low and high pumping powers, respectively, after spatial filtering through the pinhole. The red circles represent the extracted dispersion, obtained by fitting each angle-resolved linecut with a Lorentzian. The dashed lines show fits to a two-level exciton-polariton model: the black line denotes the lower polariton branch, the blue line the upper polariton branch, the green line the cavity mode, and the magenta line the heavy-hole exciton.

To confirm that this behavior is not specific to a single temperature or detuning, we repeated the measurement at 100 K for a lower-polariton exciton fraction of 0.65 (Fig. S5). A smaller pinhole of 10 $\mu$m diameter, positioned at the location indicated by the black dashed circle in Fig. S5(a,b), was used to isolate the center of the pump spot. (The image appears truncated on both sides due to the spectrometer entrance slit.) As at 80 K, the lower polariton branch remains clearly resolved both at low excitation power and at the condensation threshold, and it retains the finite curvature characteristic of the strong-coupling regime. The condensate again forms on the upper polariton branch (Fig. S5(d)).